Synthesis The Composite rGO with Zinc Oxide Nanoparticles Prepared by Cold Plasma Technology to Improving Crud Oil Derivatives .

Ola A . Ali[1],prof.Ibraheem J. Ibraheem[1]

Chemistry Department, College of Science, University of Anbar[1]

*Corresponding author (ola20s3020@uoanbar.edu.iq)

Abstract

Graphene oxide flake (GO) was preparation from graphite powder and reduced to graphene oxide (rGO) by Hydrazine hydrate.ZnONPs were prepared by cold plasma method from its salt, Zinc chloride and mixing with rGO for 24 hour to form the composite with different concentrations of metal nanoparticles. All productions are measurements doing , FTIR, UV,FAA, XRD, FE-SEM and EDX technology.Iraqi crude oil are distilled at different temperatures with composites that used as a catalyst . Our study showed remarkable results in improving oil derivatives……..

Keywords: **grapheme oxide reduced, nanoparticles, crude oil , plasma .**

DOI Number: 10.14704/nq.2022.20.10.NQ55028 **NeuroQuantology 2022; 20(10): 430-446**

Introduction

Crude oil and its derivatives are the most important sources of energy for mankind. (1)is a complicated blend of thousands of components that is difficult to fully characterize.(2) The process of separating numerous chemicals found in crude petroleum is known as petroleum refining. Atmospheric and vacuum fractional distillation is a technique in which crude oil is heated and components boil at different temperatures.(3)C atoms that have undergone sp2 hybridization are arranged in single layers in a two-dimensional honeycomb matrix to form graphite.(3)Reduced graphene oxide is manufactured from graphite by the Hammer method. In this method, graphite in first oxidized by a chemical process to produce graphene oxide, GO that contains several oxygen-containing guest groups such as -COOH, -OH, -CHO and epoxy groups. photovoltaic to reduce these aggregates and producer rGO. (4) rGO has many applications such asto increase the light absorption range and improve the photoelectrochemical (PEC) activity of TiO2.(5)and used extensively in gas sensing applications(6)

Nanomaterials are structural components with an exterior dimension in the nanoscale and a size less than 1 mm.Nanomaterials are available in a variety of forms, including spherical, tubular, and irregular.Nanomaterials can be divided into three types: nanoparticles, nanoclays, and nanoemulsions.(7-8) Different methods ,chemical, biological and physical are used to manufacture nanoparticles .Plasma is the fourth state of matter consisting of a high concentration of reactive species. Plasma is capable of changing the physical and chemical properties of the polymer surface.(9)It is a physical process of high voltage anodic deposition.(10) Thistechnology can be applied to nanomaterials such as nanofibers, nanoparticles(11)

closed neck of 500 ml and was heated at a temperature of 100 ° C in the presence of a reflective condenser for a continuous period of 24 hours. The precipitate was separated by a special filter paper, then washed with distilled water several times and with methanol CH_3OH, and then dried for 4 hours at a temperature of 70-80°C.Fourier Transform Infrared Spectroscopy (FTIR), X-ray diffraction (XRD), scanning electron microscopy(FE-SEM), and Energy Dispersive X-ray Spectroscopy (EDS) were used to characterize the produced nanocomposites .(14-15)

Preparation of zinc nanoparticles :

Zinc Oxide nanoparticles were prepared from zinc salts, cold plasma method by taking a weight of 0.7 gm of zinc chloride $ZnCl_2$ and dissolved in 100 ml of deionized water after that placed on the plasma device for 40 to 45 minutes or until the solution changed color by the action of the excited particles of Argon on the solution. Notice the color shift from transparent to yellow. Then the nanoparticles is separated by centrifugation at a speed of (12000 rpm) for 15 minutes, so we get a precipitate of zinc nanoparticles. Measurements were made using X-ray diffraction (XRD), scanning electron microscopy(FE-SEM), and Energy Dispersive X-ray (EDX).(16)

ZnO-rGOnanocomposite

The Zno-rGOnanocomposites were prepared by mixing(0.2 gm) of rGO with different concentrations of ZnO(50, 100, 150, 200, 250)PPm and added to 10 ml of methanol with continuous stirring by Magnetic stirrer for(24 hours), then separated by(12,000 cycles) centrifuge for(10 minutes), the samples were dried in the oven at(80°C).(17)

2. Methods

Synthesis and characterization GO and rGO

The graphene oxide was prepared according to the Hammer method, by adding 96 ml of concentrated sulfuric acid H_2SO_4 to a flask of capacity 1000 ml placed in an ice bath at a temperature of less than 10 ° C, then adding to it 2 gm of graphite, 1 g of sodium nitrate and 6 g of permanganate. Potassium with continuous stirring for two hours until the green color appears, then the mixture is lift from the ice bath and stirred by a magnetic stirrer for 42 hours at a temperature of 35 to 40 degrees Celsius, where the color change to brown is observed.(12-13)

The resulting solution is added to 500 ml of cooled deionized water and 5 ml of hydrogen peroxide H_2O_2 at a concentration of 30 % with continuous stirring for two hours, until the color of the solution turns light brown.The solution was separated in a centrifuge at 6000 rpm for 20 minutes each. The precipitate was washed several times with HCL at a concentration of 10%. Washing continues with deionized water until a neutral pH is reached. Then the precipitate was dried using a drying oven at a temperature of 60°C.The graphene oxide was reduced by taking 0.9 gm of oxide powder and placing it in a 500 ml beaker and adding 450 ml of distilled water, so it formed a heterogeneous suspension of graphene oxide and water was formed and this was sonicated by ultrasonic, It remained until it became a clear solution without suspension. 9 ml of hydrazine hydrate $N_2H_4.H_2O$ was added to it. After that, the mixture was transferred to a round base flask to ensure the condensation process. It contains a tightly

There are several expansion and bending bands in the range of frequencies between 400-4000 cm^{-1}, according to the FTIR spectra of graphite compounds, graphene oxide, and reduced graphene oxide.The infrared beam showed the presence of a beam centered at 3369 cm^{-1} due to (O-H) vibration in addition to the presence of symmetric and asymmetric vibration at 2843,2947cm^{-1}indicating a group (C-H), Also, the presence of a sharp peak in 1604cm^{-1} is attributed to the group (C = O).Also, many flexural and extension vibrations of the C-H group appeared in the 600-900 cm^{-1} region (figure **:**1).The infrared spectrum of graphene oxide showed the presence of a strong absorption band in 1730cm^{-1} that belongs to the organic carbonyl group (C = O), which is due to the carbonyl and carboxylic groups, and this undoubtedly indicates the formation of graphene oxideThe same spectrum also showed bands in 1026, 1207, 1309 cm^{-1}It belongs to the (C-O) organic carboxyl group, the (C-O) epoxy group, and the (C-O)aloxy grouprespectively, and this confirms the existence of a successful and clear oxidation of graphite through the use of FTIR spectrometry (figure **:2**).Infrared spectra of reduced graphene oxide were analyzed, showing a clear shift in the absorption peaks of the (O-H) group up to 3224cm^{-1} due to lack of oxygen between its molecules.Also, the value of the vibration of the (C = O) bond decreased, and this indicates a successful reduction process as the figure:(3)

Crude oil distillation

Petroleum products are distilled by a small distillation system that can distill small quantities of up to 10 ml. In the first stage, the crude oil was distilled with different stage.

1- where 300 ml of crude oil was placed in a three-mouth flask Placed on a hot plate, the sample was heated until it reached the required temperature, then the distillation was stopped temporarily to recover the distilled products, as the first distillation occurs at a temperature of 150°C, then the temperature is raised to 200°C and separated, and finally the temperature is raised to 300°C.

2-0.2 g of rGO was mixed with 300 ml of crude oil, the temperature was raised to 150 ° C, 200 ° C, and finally to 300° C and the product were collected .

3-Different weights of ZnO - rGO were added to 300 ml of crude oil for each weight and the separation was also done at different temperatures (150, 200 and 300° C).

The measurements that take place on liquids are (measuring the volume of the resulting liquid, density, viscosity, octane number, flash point,fire point and degree of aniline,) These measurements are applied to all liquid samples. (18-19)

3. RESULTS AND DISCUSSION

3.1Reduced graphene oxideIdentification

Following are some of the methods used to identify rGO.

3.1.1 Fourier Transform Infrared Spectroscopy (FTIR) for

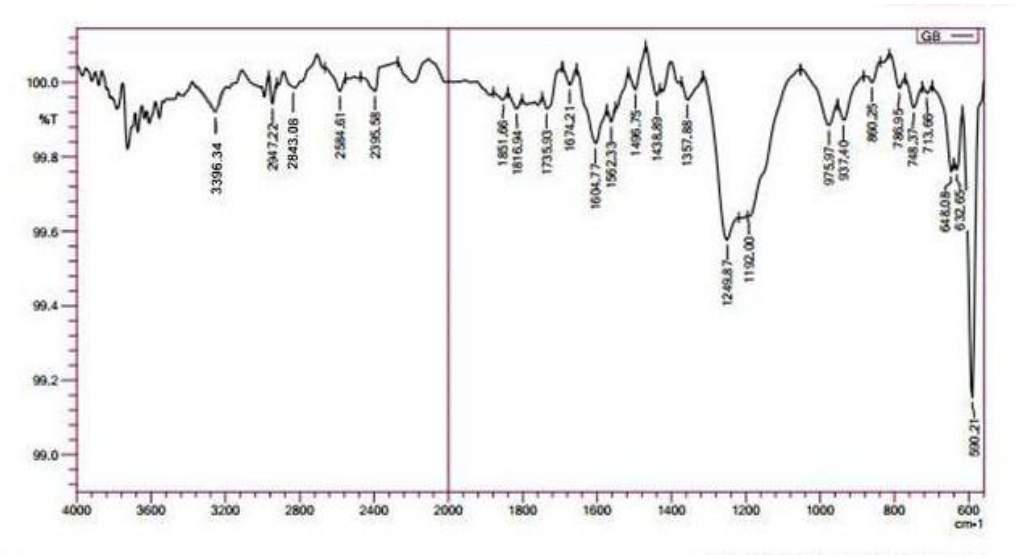

Figure (1): infrared spectrum of graphite

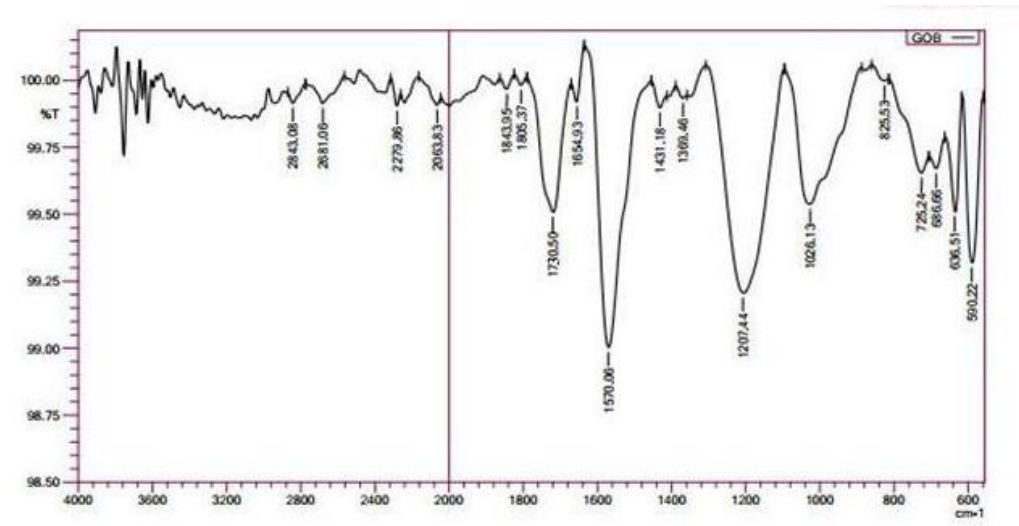

Figure (2) infrared spectrum of graphine oxide

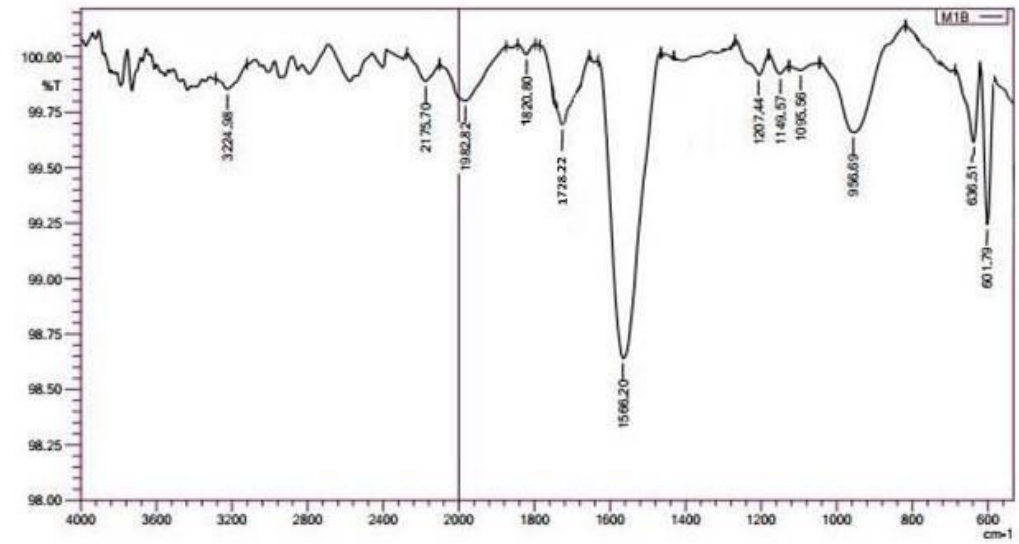

ISSN 1303-5150

Figure (3) infrared spectrum of rGO

3.1.2 The XRD analysis of rGo

The produced rGO's crystalline makeup was evaluated using XRD analysis.The XR D data of the created rGO had a 2theta degree of 10 to 80, according to Figure (4).Were at2θ (26°, 43°,and 56°,)for rGOcorresponding to Miller's indicators (111),(010),(112). The granular size was calculated according to the Debye Scherer equation and the results were according to the international card numbered (JCPDS 01-075-2078).

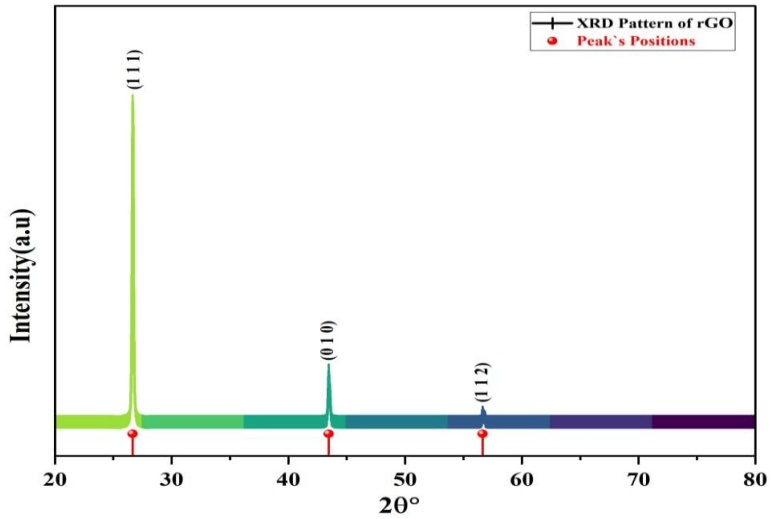

Figure (4) X-ray diffraction ofrGO

Table (1): XRD examination of rGO yielded calculated crystallite sizes for all allocated and D average peaks.

Element	2 theta	FWHM	HKI	D(nm)	Average	D average
rGO	26	0.15653	111	49.38400504	41.00485379	3.345
	43	0.19505	010	40.72950019		2.08276
	56	0.24146	112	32.90105613		1.62483

3.1.3 The FE-SEM analysis of rGO

By using FE-SEM, samples' surface morphologies can be directly identified. shows that imperfect rGO sheets exhibit a flat, wavy, and wrinkled morphology in contrast to pristine GO sheets.Additionally, the X-ray diffraction spectra revealed crystallization peaks at various angles, and the average grain size was rGO 1µm. (80.9µm, 101µm , and 111µm , 106µm)as in the figure (5) .(23-24)

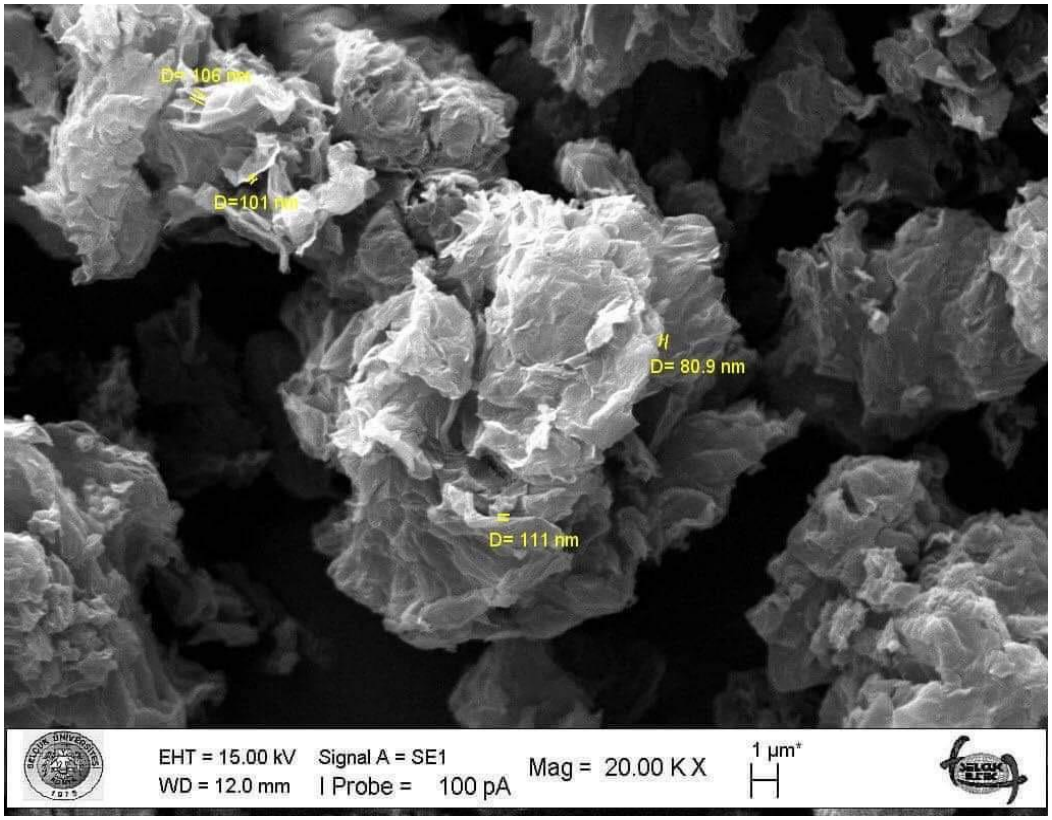

Figure (5) FE-SEM images ofrGO

3.1.4 The EDX analysis of rGO

The EDX technique was applied to the artificial sample for chemical characterisation and elemental analysis. The EDX spectrum recorded that. The table's carbon and oxygen valuesThe EDX technique was applied to the artificial sample for chemical characterisation and elemental analysis. The EDX spectrum recorded that in The table's(2) carbon and oxygen

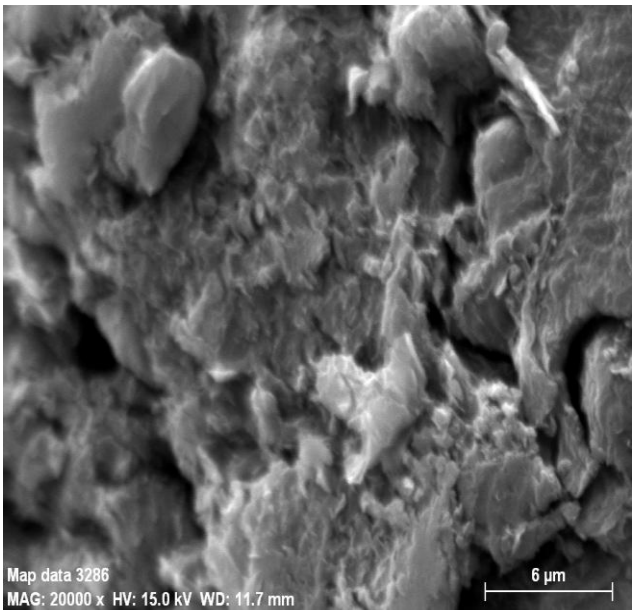

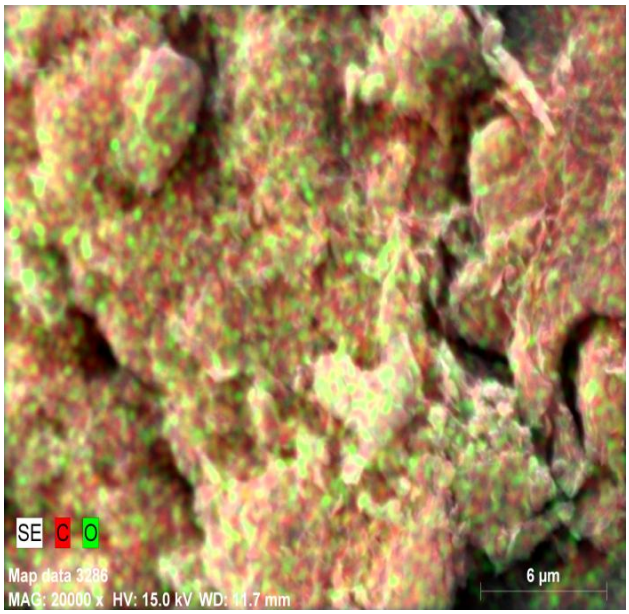

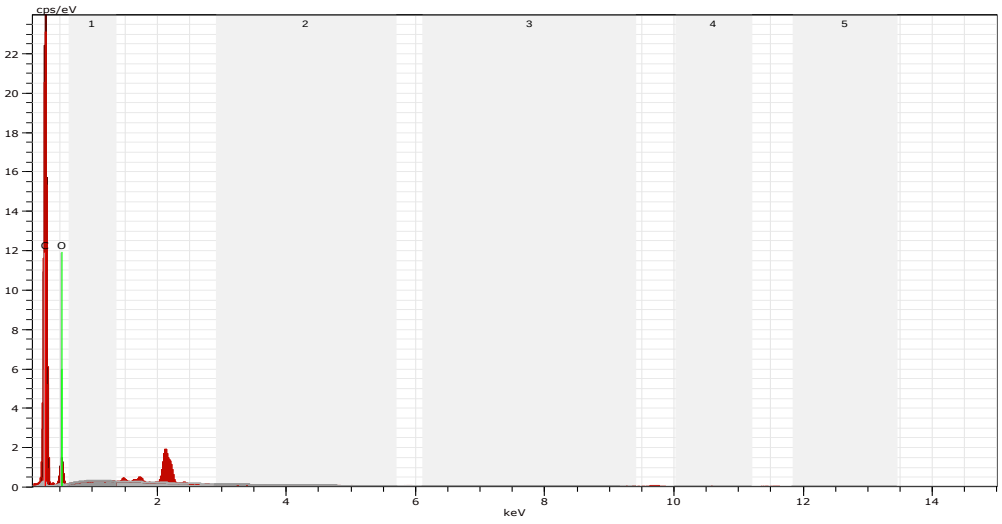

values.(25-26)

Figure (6) EDX spectrum ofrGO

Table (2): EDX examination of rGO

Element	Series	unn. C [wt.%]	norm. C [wt.%]	Atom. C [at.%]	Error [%]
Carbon	K-series	70.34	70.34	75.96	21.5
Oxygen	K-series	29.65	29.66	24.04	9.5
Total:		100.00	100.00	100.00	

4.zinc Oxide nanoparticles Identification

Several methods were used to identify zno NPs, as follows:

4.1.Uv-visible of Zinc Oxide nanoparticles

A technique that may verify the synthesis of metal is UV-Vis spectroscopy.Figure(7) provides the zno solution's UV-Vis spectrumPrepared by cold plasma technologyUV-visible spectroscopy has identified the specific nanoparticle formation during color change from the absorption spectra.(27-28) and the room temperature UV visible absorption spectrum of ZnO nanoparticles was measured in the wavelength range 200-800 nmThe spectrum has a peak at 368 nm which can be assigned to the intrinsic band-gap absorption of ZnO due to the electron transitions from the valence band to the conduction band (O2p → Zn3d). In addition, this sharp peak shows that the particles are innano size and the particle size distribution is narrow.(29)

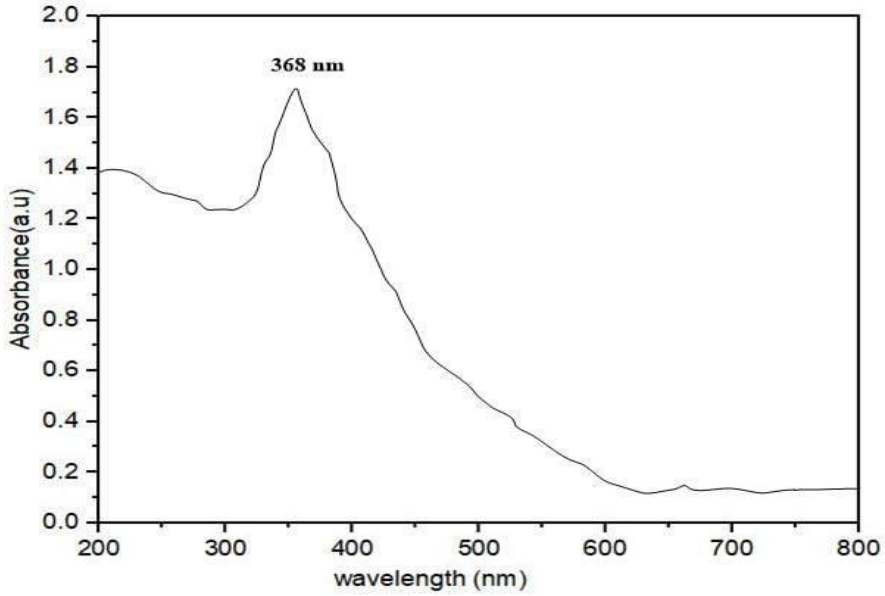

Figure (7): UV-Vis spectrum of ZnONPs

4.2.The XRD analysis of Zinc Oxide nanoparticles

The crystalline makeup of the produced zno NPs was evaluated using XRD analysis.The produced ZnO NPs' XRD data are shown in Figure (8).The 2theta degree of ZnONPs ranged from 10 to 80, and strong peaks were found atat2θ(31°, 34°, 47°, 56°, 66°, 67°,and 76°)which corresponded tothe HKI(100), (002), (102), (110), (200), (112), and (202)respectively, according to (JCPDS: 98-005-7478).(30-31)

Figure (8) X-ray diffraction ofZnO NPs

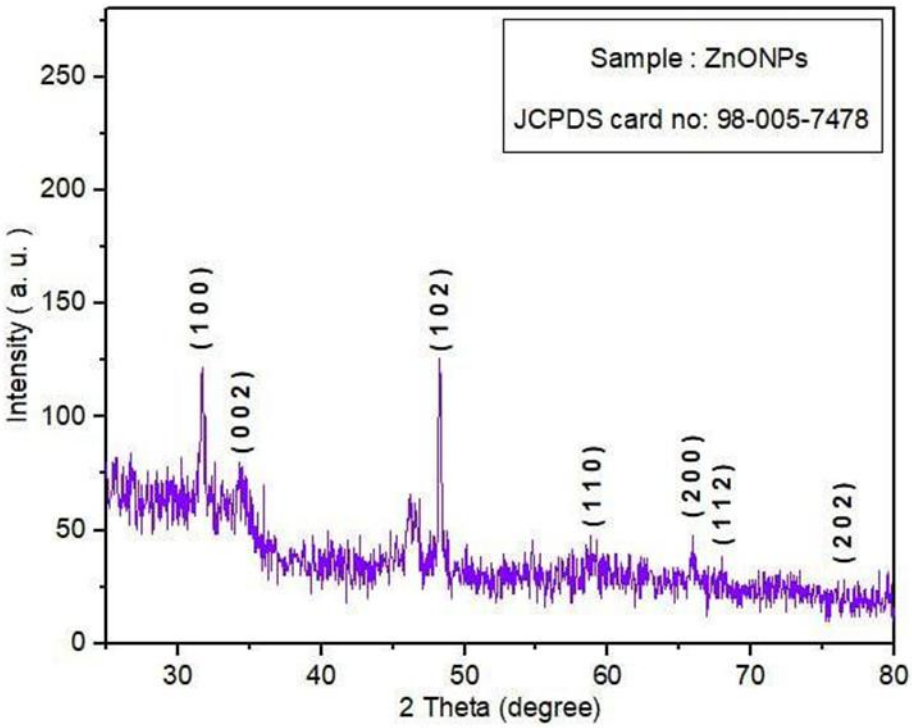

ISSN 1303-5150

Table (3): XRD examination of ZnO yielded calculated crystallite sizes for all allocated and D average peaks.

Element	2 theta	FWHM	**HKI**	D(nm)	Average	D average
zno	**31**	**0.2952**	**100**	**26.3689**73	**26.51386367**	**3.86618**
	34	**0.2952**	**002**	**25.87227459**		**2.80098**
	47	**0.5904**	**102**	**12,83828532**		**2.57232**
	56	**0.7872**	**110**	**9.298159603**		**1.98337**
	66	**0.1968**	**200**	**36.85586001**		**1.88872**
	67	**0.1476**	**112**	**47.84965521**		**1.68328**
	76	**0.3936**	**202**	**16.94181757**		**1.41758**

4.3.The FE-SEM analysis ofZinc Oxide nanoparticles

ZnO NPs clearly show that nanopowders are aggregated crystals with almost uniform spherical shapes.(32) A picture SEM of ZnO NPs taken using scanning electron microscopy is shown in (Figure:9). The ZnO nanoparticles' crystallinity was linked, and the morphology of grains of approximately same size was observed. Using the SEM analytical technique, the surface morphologies of produced ZnO powders were examined, revealing shape and uniform size distributions for ZnO NPs This confirms the EDX analysis that showed the presence of the element oxygen and zinc.where he appeared the average grain size for ZNO NPs (33.4 nm , 41.9 nm , 44.9 nm) .(33)

Figure (9):SEM spectrum of ZNO NPs

4.4.The TEM analysis of Zinc Oxide nanoparticles

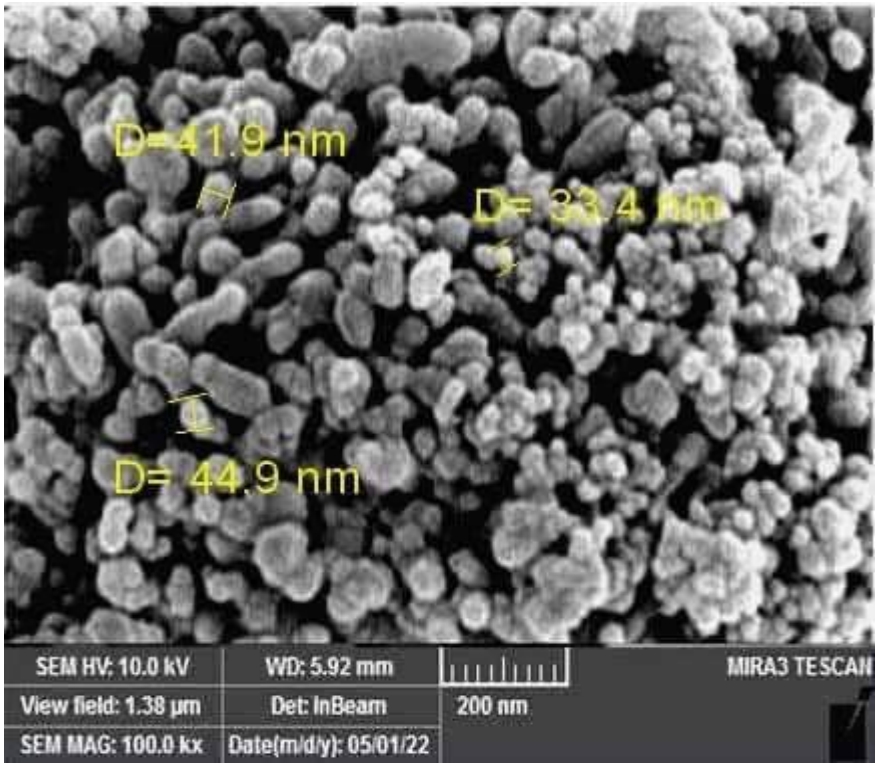

The transmission electron microscope analysis (TEM) was used to measure the size, shape, and morphological characteristics of ZnONPsThe morphology and dimensions of the biosynthesisedZnO nanoparticles were initially described by transmission electron microscopic (TEM) images (figure: 10), and the estimated ZnO nanoparticle size from TEM images revealed that they had various shapes, primarily irregular tiny spherical onest was her size (57.3 nm , 112.5 nm).

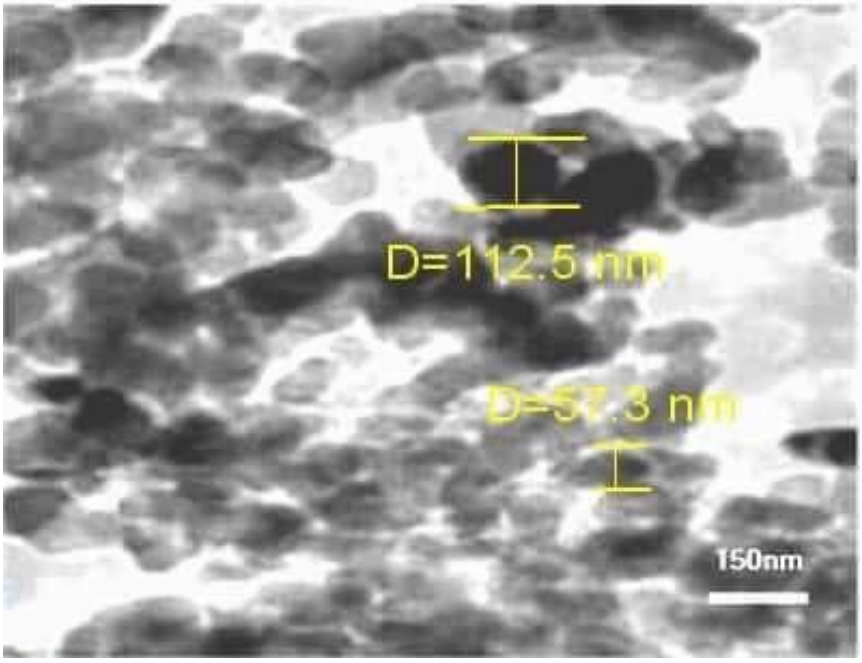

Figure (10). TEM for ZNO NPs

4.5.The EDX analysis ofZinc Oxide nanoparticles

EDX spectra provide information on the ZnO-NPs' elemental makeup.The existence of zinc oxide nanoparticles was confirmed by the EDX examination. Strong signal energy peaks were visible in the spectra for zinc (Zn) atoms and a weak signal energy peak for oxygen (O). This attests to the existence of zinc in the form of oxide.Weak peaks of Chlorine, Iron, Carbon and Chromium were also observed due to the presence of impurities in the material or contamination from the plasma electrodeand the instrumentsas in the table(4).(35-36-37)

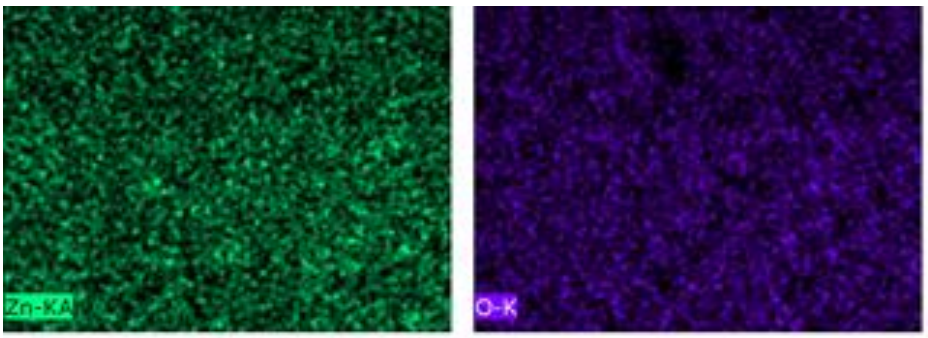

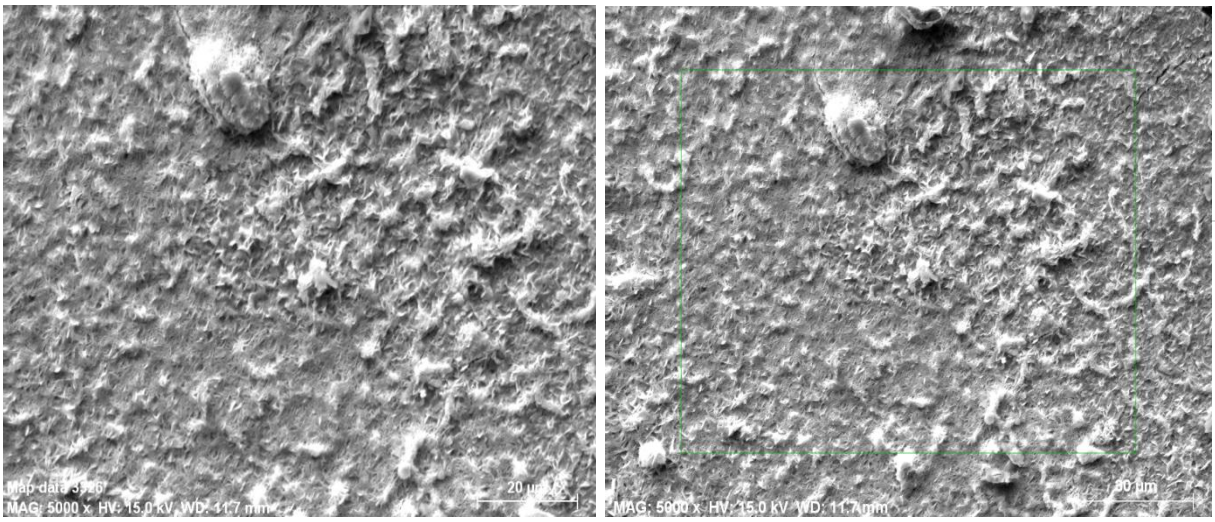

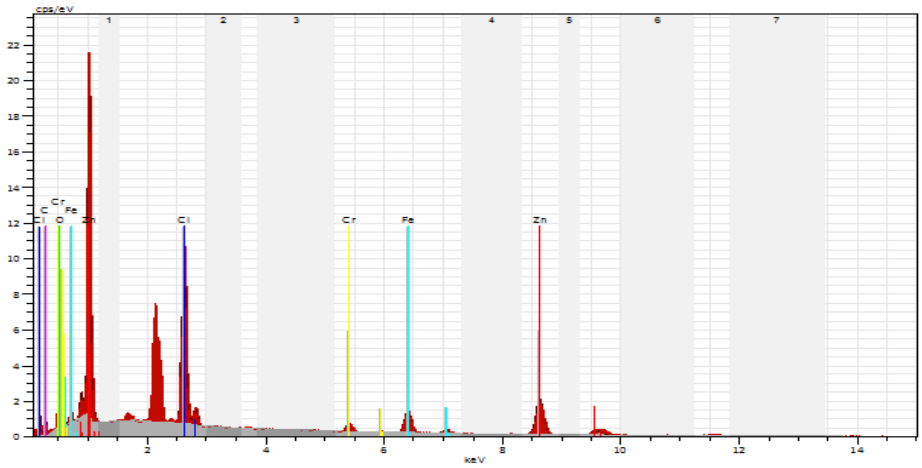

Figure (10) EDX spectrum of ZNO NPs

Table (4): XRD examination of ZnO

Element	Series	unn. C [wt.%]	norm. C [wt.%]	Atom. C [at.%]	Error [%]
Zinc	K-series	32.15	49.27	25.98	1.1
Oxygen	K-series	12.06	18.48	39.84	1.7
Chlorine	K-series	10.63	16.29	15.84	0.4
Iron	K-series	6.48	9.93	6.13	0.2
Carbon	K-series	2.43	3.72	10.67	0.5
Chromium	K-series	1.51	2.31	1.53	0.1
Total:		65.25	100.00	100.00	

Characteristics of distilled at 150°C gasoline								
eter	ne		oil	+50 zn				Concl
Characteristics of distilled at 200°C kerosene								
RON	95.3	78.9	79.6	54.9	86.5	95.9	96.4	96.8
MON	85.3	76.3	76.5	51.9	66.8	76.8	76.3	76.8
AKI	90.3	77	78	53.4	67	78.3	78.8	78.3
density	0.7364	0.5747	0.6843	0.5741	0.6502	0.5659	0.61653	0.5791
viscosity	1.264	0.3193	0.4529	0.2859	0.4092	0.3144	0.3356	0.2931
volum		25	10	34	15	32	34.5	36
Flash point	22	25	23	29	24	25	31	30
Fire point	25	29	25	31	27	28	35	35
Aniline point	100	105	130	133	138	105	103	100
API	60.6510	114.7154	75.2655	114.9383	86.1052	118.5441	98.0103	119.8235
tft	-21.2	-49.1	--	-42.1	--	-69.5	-47.6	-69.7
typ	w	s	s	A	S	A	A	A

parameter	kerosene	Crude oil	Crud oil +rGO	Oil+rGO+ 50 zn	+100zn	150 zn	200zn	250zn
RON	97.4	65.3	93.8	91.3	87.5	92.1	94.9	95.5
MON	87.4	62.2	84	82.7	64.5	83.1	82.9	82.7
AKI	92.4	63.5	88	87	66.3	87.1	87.4	87.1
density		0.7065	0.7298	0.73206	0.6865	0.7099	0.7013	0.6858
viscosity		0.5191	0.5474	0.4508	0.5475	0.5216	0.4798	0.4528
volum		27	27.5	23ML	23	28	28.5	29
Flash point		26	25	41	23	26	28	22
Fire point		28	28	46	26	29	34	26
Aniline point		115	135	135	140	115	120	115

API		68.7830	62.3860	61.7901	74.6089	67.8154	70.2681	
tft	-5.2	-29	-30.8	-42.1	-46	-37	-38.5	-43.3
typ	S	S	W	A	A	W	A	A

Characteristics of distilled at 300°C diesel

		oil	**oil +rGO**	**O+0.6zn**				
density		0.7699	0.7320	0.7702	0.7783	0.7770	0.7645	0.7840
viscosity		0.8686	0.8885	0.8102	0.8243	0.8766	0.9132	0.9486
volum		63	80	85.5	55.5	51	53	60.5
Flash point		54	62	56	54	54	55	50
Fire point		58	78	68	62	58	62	60
Aniline point		130	156	159	156	130	153	155
API		52.2901	61.7972	52.2185	50.3041	50.5966	53.5882	48.9846
CET	52.2	53.5	53.6	53.5	53.4	53.3	53.4	54.4
tft	-28.2	-20	-18.09	-20.02	-21	-21.5	-21.4	-21.2
typ	w	w	s	w	w	w	w	W
Cet+kerosen								
typ	s	s	s	s	s	s	s	s
K	7.1%	0.0%	0.0%	0.0%	0.0%	0.0%	0.0%	0.0%

Characteristics of distilled at 150°C+200

	ne	oil	Oil+rGO	O+50zn	+	zn	+	
OCTAN								
T	34.2	29.6	30.4	33.2	28.6	35.8	34.3	29.5
Ron	97.4	S	94.3	92.3	92.3	91.6	91.9	91.7
Mon	87.4	0.0%	84.3	83.3	83.3	82.8	82.9	82.3
AKI	92.4	87.3	89.3	87.8	87.8	87.2	87.4	87.1
Tft	-5.2	-39.6	-28.9	-34.8	-36.2	-41.7	-38.8	-42
Typ	S	A	W	W	W	A	A	A
Volume		52	37.5	57	38	60	47	51
Density		0.7483	0.7488	0.7168	0.7703	0.6574	0.7333	0.6983
Viscosity		0.4229	0.5305	0.7613	0.6163	0.4935	0.5387	0.5115

API		57.5952	57.4690	65.9051	52.1827	83.7418	61.4633	71.1204
Flash point		18	35	15	25	27	25	14
Fire point		21	25	20	35	25	23	18
Aniline point		120	118	120	120	130	112	119

In this work, GO was synthesized using Hummer method and reduced to rGO using hydrazine. and combined with zinc oxide nano-zinc oxide zno-rGO prepared from zinc salt by cold plasma method.The properties of rGO ZNO compounds were characterized using spectroscopy, X-ray diffraction, and microscopy techniques.The zno-rGOnanocomposit was used with Iraqi crude oil. The nanocomposites showed remarkable results in enhancing the energy values of some petroleum derivativesWhere the following was produced:

1-Characteristics of distilled at 150°C gasolin (petrol)

-Its size varies with a clear increase with increasing nano concentration

-A decrease in the degree of aniline with an increase in the concentration of nanoparticles indicates an increase in the aromatic content.

-A clear increase in the API value, which indicates the hidden product

- A significant decrease in the value of the tft (cloud point) indicates a lack of wax

-This makes its density and viscosity low and type A, which means that it can be used in the frozen pole

-An increase in RON value with a slightly higher Nano concentration makes it an improved fuel

- The value of the MON is low with a small increase in the concentration of nanoparticles, but it does not amount to gasoline fuel

2- Characteristics of distilled at 200°C kerosene

-Its size varies with a clear increase with increasing nano concentration

-The degree of aniline is higher than the distilled at 150 with a slight decrease with the increase in the nano concentration

- The API value is less than the distillate value at 150, which indicates that it is less subtle than the distillate at 150

- An increase in the tft value of the distillate at 150, but it remains of the polar type. This indicates a small increase in the wax content, as well as in the viscosity and density

- An increase in the value of O.N with an increase in the nano concentration, but it remains a fuel with low energy content.

3- Characteristics of distilled at 300°C diesel

-The quantity is twice the volume of the distillate at 150 and 200 degrees with a slight decrease with an increase in the nano concentration.

- A high rise in the value of the degree of aniline with an increase in the concentration of nanoparticles, which indicates an increase in the paraffinic content.

- A high degree of aniline value with a low concentration of nanoparticles, which indicates an increase in the paraffinic content

- A significant decrease in the API value with an increase in the nano concentration, which indicates an increase in the weight of the product and this is evident in the density and viscosity value.

- An increase in the value of TFT, and this indicates an increase in the amount of wax and type W of winter fuel
- An increase in the value of cet by increasing the concentration of nanoparticles, which makes it a good fuel
- The value of k is 0.0% and this makes it a more pure fuel.

4-Characteristics of distilled at 150°C+200

-Significant increase in volume due to mixing

-A decrease in the degree of aniline with an increase in the concentration of nanoparticles indicates an increase in the aromatic content.

- A clear increase in the API value, which indicates the hidden product

-A significant decrease in the value of the tft (cloud point) indicates a lack of wax

- This makes its density and viscosity low and type A, which means that it can be used in the frozen pole

- The O.N value is low with a small increase in the nano concentration, but it remains a fuel and a low energy content.

References

1-Olivares-Rubio, H. F., & Espinosa-Aguirre, J. J. (2021). Acetylcholinesterase activity in fish species exposed to crude oil hydrocarbons: A review and new perspectives. *Chemosphere*, *264*, 128401.

2-Banda-Cruz, E. E., Gallardo-Rivas, N. V., Martínez-Orozco, R. D., Páramo-García, U., & Mendoza-Martínez, A. M. (2021). Derivative UV-Vis Spectroscopy of Crude Oil and Asphaltene Solutions for Composition Determination. *Journal of Applied Spectroscopy*, *87*(6), 1157-1162.

3-Liu, G., Yan, B., & Chen, G. (2013). Technical review on jet fuel production. *Renewable and Sustainable Energy Reviews*, *25*, 59-70.

4-Islam, F., Tahmasebi, A., Wang, R., & Yu, J. (2021). Structure of coal-derived metal-supported few-layer graphene composite materials synthesized using a microwave-assisted catalytic graphitization process. *Nanomaterials*, *11*(7), 1672.

5-Mondal, A., Prabhakaran, A., Gupta, S., & Subramanian, V. R. (2021). Boosting photocatalytic activity using reduced graphene oxide (RGO)/semiconductor nanocomposites: issues and future scope. *ACS omega*, *6*(13), 8734-8743.

6-Hajialilou, E., Asgharzadeh, H., &Asl, S. K. (2021). TiO2/rGO/Cu2O ternary hybrid for high-performance photoelectrochemical applications. *Applied Surface Science*, *544*, 148832.

7-Majhi, S. M., Mirzaei, A., Kim, H. W., & Kim, S. S. (2021). Reduced graphene oxide (rGO)-loaded metal-oxide nanofiber gas sensors: An overview. *Sensors*, *21*(4), 1352.

8-Sircar, A., Rayavarapu, K., Bist, N., Yadav, K., & Singh, S. (2021). Applications of nanoparticles in enhanced oil recovery. *Petroleum Research*.

9-Liu, D., Zhang, X., Tian, F., Liu, X., Yuan, J., & Huang, B. (2022). Review on nanoparticle-surfactant nanofluids: Formula fabrication and applications in enhanced oil recovery. *Journal of Dispersion Science and Technology*, *43*(5), 745-759.

10-Naebe, M., Haque, A. N. M. A., & Haji, A. (2021). Plasma-assisted antimicrobial finishing of textiles: A review. *Engineering*.

11-Naebe, M., Haque, A. N. M. A., & Haji, A. (2021). Plasma-assisted antimicrobial finishing of textiles: A review. *Engineering*.

12-Ucar, Y., Ceylan, Z., Durmus, M., Tomar, O., &Cetinkaya, T. (2021). Application of cold plasma technology in the food industry and its combination with other emerging technologies. *Trends in Food Science & Technology*, *114*, 355-371.

Codistillation: A Detailed Characterization Study by FTICR Mass Spectrometry. *Energy & Fuels*, *35*(17), 13830-13839.

20-Kumar, R., Maheshwari, S., Voolapalli, R. K., &Upadhyayula, S. (2021). Investigation of physical parameters of crude oils and their impact on kinematic viscosity of vacuum residue and heavy product blends for crude oil selection. *Journal of the Taiwan Institute of Chemical Engineers*, *120*, 33-42.

21-Koçanalı, A., &ApaydınVarol, E. (2021). An experimental study on the electrical and thermal performance of reduced graphene oxide coated cotton fabric. *International Journal of Energy Research*, *45*(9), 12915-12927.

22-Kumar, N. S., Al-Ghurabi, E. H., Asif, M., &Boumaza, M. (2021). Retrieving and morphological portrayal of Cu-nanoparticle impregnated reduced graphene oxide (CuNP@ rGO) electrochemical bio-sensor. *Sensors and Actuators A: Physical*, *329*, 112826.

23-Tewatia, K., Sharma, A., Sharma, M., & Kumar, A. (2021). Synthesis of graphene oxide and its reduction by green reducing agent. *Materials Today: Proceedings*, *44*, 3933-3938.

24-Zhao, R., Li, Y., Ji, J., Wang, Q., Li, G., Wu, T., & Zhang, B. (2021). Efficient removal of phenol and p-nitrophenol using nitrogen-doped reduced graphene oxide. *Colloids and Surfaces A: Physicochemical and Engineering Aspects*, *611*, 125866.

25-Elbasuney, S., El-Sayyad, G. S., Tantawy, H., &Hashem, A. H. (2021). Promising antimicrobial and antibiofilm activities of reduced graphene oxide-metal oxide (RGO-NiO, RGO-AgO, and RGO-ZnO) nanocomposites. *RSC advances*, *11*(42), 25961-25975.

13-Rasheed, M., Shihab, S., & Sabah, O. W. (2021, March). An investigation of the structural, electrical and optical properties of graphene-oxide thin films using different solvents. In *Journal of Physics: Conference Series* (Vol. 1795, No. 1, p. 012052). IOP Publishing.

14-Varaprasad, D., Raghavendra, P., Sudha, N. R., Sarma, L. S., Parveen, S. N., Chandana, P., ... & Chandrasekhar, T. (2022). Bioethanol production from green alga Chlorococcumminutum through Reduced graphene oxide-supported platinum-ruthenium (Pt-Ru/RGO) nanoparticles. *BioEnergy Research*, *15*(1), 280-288.

15-Guo, J., Mao, B., Li, J., Wang, X., & Yang, X. (2021). Rethinking the reaction pathways of chemical reduction of graphene oxide. *Carbon*, *171*, 963-967.

16-Dash, B. S., Jose, G., Lu, Y. J., & Chen, J. P. (2021). Functionalized reduced graphene oxide as a versatile tool for cancer therapy. *International Journal of Molecular Sciences*, *22*(6), 2989.

17-Qin, L., Takeuchi, N., Takahashi, K., Kang, J., Kim, K. H., & Li, O. L. (2021). N2/Ar plasma-induced surface sulfonation on graphenenanoplatelets for catalytic hydrolysis of cellulose to glucose. *Applied Surface Science*, *545*, 149051.

18-Jilani, A., Hussain, S. Z., Ansari, M. O., Kumar, R., Dustgeer, M. R., Othman, M. H. D., ... &Melaibari, A. A. (2021). Facile synthesis of silver decorated reduced graphene oxide@ zinc oxide as ternary nanocomposite: an efficient photocatalyst for the enhanced degradation of organic dye under UV–visible light. *Journal of Materials Science*, *56*(12), 7434-7450.

19-Chiaberge, S., Siviero, A., Passerini, C., Pavoni, S., Bianchi, D., Haider, M. S., &Castello, D. (2021). Co-processing of Hydrothermal Liquefaction Sewage Sludge Biocrude with a Fossil Crude Oil by

ISSN 1303-5150

investigation of green synthesized silver and zinc oxide nanoparticles. *Journal of Inorganic and Organometallic*

34-El-Hawwary, S. S., AbdAlmaksoud, H. M., Saber, F. R., Elimam, H., Sayed, A. M., El Raey, M. A., &Abdelmohsen, U. R. (2021). Green-synthesized zinc oxide nanoparticles, anti-Alzheimer potential and the metabolic profiling of Sabalblackburniana grown in Egypt supported by molecular modelling. *RSC advances*, *11*(29), 18009-18025.

35-Faisal, S., Jan, H., Shah, S. A., Shah, S., Khan, A., Akbar, M. T., ... & Syed, S. (2021). Green synthesis of zinc oxide (ZnO) nanoparticles using aqueous fruit extracts of Myristicafragrans: their characterizations and biological and environmental applications. *ACS omega*, *6*(14), 9709-9722.

36-Ekennia, A., Uduagwu, D., Olowu, O., Nwanji, O., Oje, O., Daniel, B., ... & Emma-Uba, C. (2021). Biosynthesis of zinc oxide nanoparticles using leaf extracts of Alchornealaxiflora and its tyrosinase inhibition and catalytic studies. *Micron*, *141*, 102964.

37-Jayachandran, A., Aswathy, T. R., & Nair, A. S. (2021). Green synthesis and characterization of zinc oxide nanoparticles using Cayratiapedata leaf extract. *Biochemistry and Biophysics Reports*, *26*, 100995.

38-Khurana, N., Arora, P., Pente, A. S., Pancholi, K. C., Kumar, V., Kaushik, C. P., & Rattan, S. (2021). Surface modification of zinc oxide nanoparticles by vinyltriethoxysilane (VTES). *Inorganic Chemistry Communications*, *124*, 108347.

26-Korkmaz, S., Kariper, İ. A., Karaman, O., &Karaman, C. (2021). The production of rGO/RuO2 aerogel supercapacitor and analysis of its electrochemical performances. *Ceramics International*, *47*(24), 34514-34520.

27-Siddique, S., Waseem, M., Naseem, T., Bibi, A., Hafeez, M., Din, S. U., ... &Qureshi, S. (2021). Photo-Catalytic and Anti-microbial Activities of rGO/CuONanocomposite. *Journal of Inorganic and Organometallic Polymers and Materials*, *31*(3), 1359-1372.

28-Zinc Oxide Nanoparticles: from Biosynthesis, Characterization, and Optimization to Synergistic Antibacterial Potential

29-Green synthesis and characterization of biocompatible zinc oxide nanoparticles and evaluation of its antibacterial potential

30-Jayachandran, A., Aswathy, T. R., & Nair, A. S. (2021). Green synthesis and characterization of zinc oxide nanoparticles using Cayratiapedata leaf extract. *Biochemistry and Biophysics Reports*, *26*, 100995.

31-El-Hawwary, S. S., AbdAlmaksoud, H. M., Saber, F. R., Elimam, H., Sayed, A. M., El Raey, M. A., &Abdelmohsen, U. R. (2021). Green-synthesized zinc oxide nanoparticles, anti-Alzheimer potential and the metabolic profiling of Sabalblackburniana grown in Egypt supported by molecular modelling. *RSC advances*, *11*(29), 18009-18025.

32-Rajput, V. D., Minkina, T., Fedorenko, A., Chernikova, N., Hassan, T., Mandzhieva, S., ... &Burachevskaya, M. (2021). Effects of zinc oxide nanoparticles on physiological and anatomical indices in spring barley tissues. *Nanomaterials*, *11*(7), 1722.

33-Vinay, S. P., & Chandrasekhar, N. (2021). Structural and biological

ISSN 1303-5150